Investigations on structural and optical properties of co-doped (Ag, Co) ZnO nanoparticles

B. SANKARA REDDY, S. VENKATRAMANA REDDY*, P. VENKATESWARA REDDY, N. KOTEESWARA REDDY[a]
Department of Physics, Sri Venkateswara University, Tirupati 517502, A.P, India
[a]Center for Nanoscience and Engineering (CeNSE), Indian Institute of Science, Bangalore-560 012, India

Undoped and co-doped (Ag, Co) ZnO powders were synthesized by chemical co-precipitation method without using any capping agent. The X-ray diffraction results indicate that the undoped and co-doped ZnO powders have pure hexagonal structure and are consisting of nanosized single-crystalline particles. The size of the nanoparticles increases with increasing Ag concentration from 1 to 5 mol% as compared to that of undoped ZnO. The presence of substitution dopants of Ag and Co in the ZnO host material was confirmed by the Energy dispersive analysis of X-rays (EDAX). Optical absorption measurements indicate blue shift and red-shift in the absorption band edge upon doping concentration of Ag and blue emission was observed by photoluminescence (PL) studies.

(Received July 23, 2012; accepted October 30, 2012)

Keywords: ZnO nanoparticles, Co-precipitation method, Structural properties, Optical properties, EDS (EDAX)

1. Introduction

In recent years nanostructure materials have plays an important role in the various research fields, because of their unique physical properties and novel potential applications. Among II-VI semiconductors, Zinc oxide (ZnO) is one of the best host materials and an important technological material for room temperature UV- lasers and the development of various optoelectronic devices because it has a wide direct band gap of 3.37 eV and a large exciton binding energy 60 meV [1-4]. Furthermore, ZnO can be used in many applications such as photoconductors, integrated sensors and transparent conducting oxide electrodes [5], piezoelectric sensors [6], gas sensors [7] solar cell applications [8] because of its unique electrical and optical properties. The shape of the ZnO nanoparticles depends on the reaction conditions during their formation, and many methods have been used to synthesize ZnO nanoparticles, for example sol-gel [9], hydrothermal [10], and chemical co-precipitation [11,12]. Nowadays many of the researchers used some elements such as alkali, alkaline earth, transition metal and rare earth elements [13-16]. In this concern much effort has been devoted to the doping of ZnO nanocrystals. ZnO based materials with silver (Ag) [17-20] and also ZnO based materials with cobalt (Co) [21-24] extend their potential applications found that its microstructure, morphology and luminescence performance extremely sensitive to the conditions of their preparation. In this paper, we report the changes of ZnO nanostructures morphology induced by silver (by keeping Co = 5.0 mol% concentration as constant). By using chemical co-precipitation method undoped ZnO and $Zn_{1-x}Ag_xCo_yO$ (x = 0.00 to 0.05, y = 0.00 and 0.05) nanostructures were synthesized [25] and their structural, morphology, and optical properties have been investigated.

2. Experimental

Pure ZnO nanocrystals were synthesized by chemical co-precipitation method at 40^0C temperature by using zinc acetate dehydrate (Zn $(CH_3COO)_2$ $2H_2O$) and potassium hydroxide (KOH) as precursors and for cobalt and silver doping cobalt acetate (Co $(C_2H_3O_2)_2$) and silver nitrate ($AgNO_3$) have been used. $Zn_{1-x}Ag_xCo_yO$ (x = 0.00 to 0.05, y = 0.00 and 0.05) nanostructures were prepared at 40^0C temperature as the procedure described below.

Initially 0.2 M solution was prepared by using zinc acetate and KOH. Dopant silver nitrate has been added drop-wise to the above solution in different concentrations varied from 1-5 mol% by keeping cobalt acetate concentration as constant, 5 mol % under continuous stirring for 10 hrs. After the precipitate was filtered out separately and repeatedly washed with deionized water to remove unnecessary impurities formed during the preparation process. Co and Ag doped ZnO powders were obtained after drying at 70^oC for 9 hrs. Then the final products were grinded and annealed at 500^oC in the furnace for 1 hr.

The structural properties including structure and crystallite size of the samples were determined by Seifert 3003 TT X-ray diffractometer (XRD) using CuK_α radiation by applying voltage and current of 40 kV and 30 mA respectively. Morphology of the powders was studied by field emission scanning electron microscopy (FE-SEM) (Model: ZEISS ULTEA 55, Gemini). Concentration of dopants in ZnO was estimated by energy dispersive X-ray

spectroscopy (EDS) attached with SEM (Model: CARL-ZEISS EVOMA 15). UV-DRS (diffuse reflectance spectroscopy) spectra were recorded on a Varian UV−vis spectrometer in the wavelength range of 200−800 nm, and photoluminescence (PL) studies were carried out using PL spectrometer (Model: OBINYOUN fluorolog-3) with a 450 W Xenon arc lamp as an excitation source.

3. Results and discussion

3.1 Structural properties of the pure ZnO and $Zn_{1-x}Ag_xCo_yO$ nanoparticles

Typical XRD patterns of ZnO and $Zn_{1-x}Ag_xCo_yO$ powders are shown in Fig. 1. The diffraction peaks of all samples are quite matching with the hexagonal wurtzite structure of ZnO data [JCPDS 36-1451]. No traces of impurity peaks are observed. The crystallite sizes of the synthesized powders are estimated from X-ray lines broadening using Scherer's equation $D = \frac{0.89\,\lambda}{\beta \cos\theta}$, where 'β' is full width at half maximum (FWHM), 'θ'-diffraction angle, and 'λ'-wavelength of X-rays [26]. In past study, transition elements like Co doped ZnO nanoparticles, with increase in dopant concentration of 'Co', the average particles size may decrease or increase, the lattice constants are decreased or increased and the position of the X-rd peaks shifted towards lower or higher '2θ' value. Such changes also suggests that most of the 'Co' ions with smaller ionic radii (0.065 nm) substitute Zn ions (0.074 nm) in the ZnO lattice and in some cases Co doped ZnO doesn't show any change in lattice parameters, particles size and position of the X-rd peaks as reported in literature [27-31]. The diffracted intensity and size of the particles increases with increase of 'Co' concentration and hence the lattice parameters decreases [32, 33]. Also in 'Ag' doped ZnO nanoparticles, the X-rd peak positions moves towards lower angle, because of atomic radii of Zn^{2+} is lesser than the Ag^{+}. The average particles size decreased or increased, diffracted intensity decreased by increasing doping concentration of Ag [12, 19, and 34]. However, we used two transitional elements such as Ag, Co, which are co-doped in ZnO nanoparticles; we observed that there is no change of X-rd peak positions of $Zn_{1-x}Ag_xCo_yO$ nanoparticles. Thus, we may conclude that the diffracted intensity, particles size increases and hence lattice constants are decreased by increasing dopant concentration of Ag for the following reason. The ionic radius of Ag^{+} (0.122nm) is greater than the ionic radii of Zn^{2+} (0.088nm) and also, the ionic radii of Co^{2+} (0.065 nm) is smaller than the ionic radii of Zn^{2+}. The evaluated particle sizes and lattice constants of the samples are given in Table 1. Intensity point of view, the diffracted intensity of Ag doped ZnO nanoparticles increases by increasing of Ag concentration from 1-5 mol% (by keeping Co = 5 mol %). The diffracted intensities of all concentrations of Ag doped ZnO nanoparticles shows higher intensity than the pure ZnO and is clearly noticed from Fig. 1. The enhanced intensities of the XRD peaks of co-doped ZnO samples suggest better crystallinity. However, the evaluated bond length (l) and lattice parameters (a, and c are given in Table 1) of ZnO gradually decrease with increasing dopant concentration of Ag (by keeping Co = 5.0 mol %). To see the effect of doping on Zn-O bond length, bond length (l) has been calculated using the following formula [35].

$$l = \sqrt{\frac{a^2}{3} + \left(\frac{1}{2} - u\right)^2 c^2} \quad (1)$$

where **a** and **c** are the lattice parameters and

$$u = \frac{a^2}{3c^2} + 0.25$$

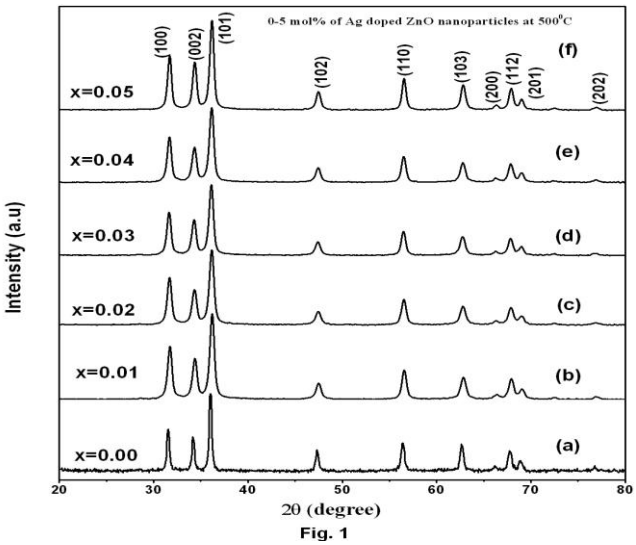

Fig. 1

Fig. 1. X-rd pattern of: (a) Pure ZnO (b) 1 mol% Ag doped (c) 2 mol % Ag doped, (d) 3 mol% Ag doped, (e) 4 mol% Ag doped, and (f) 5 mol % Ag doped ZnO nanoparticles.

Table 1. Bond length (L), particle size (D), and lattice parameters LP (a and c) of pure and co-doped ZnO samples.

Ag(mol%) concentration	L(nm)	D(nm)	LP(nm)	
			a	c
Undoped	0.199032	23	0.326183	0.523822
1	0.198272	44	0.325661	0.521575
2	0.198219	50	0.325228	0.522164
3	0.198201	58	0.324927	0.522755
4	0.198099	57	0.324722	0.522459
5	0.197637	58	0.324630	0.520693

3.2 Morphology and elemental studies of the nanoparticles

Field emission Scanning electron microscope (FE-SEM) was used to investigate the morphology of the samples as shown in the Fig. 2. Undoped ZnO image appears like the shape of cauliflower (Fig. 2(a)) and 5 mol% of Ag + 5 mol% of Co doped ZnO nanoparticles forms the quasispherical shape (Fig. 2(b)), all these particles present in the size of 100 nm. Fig. 3 depicts the energy dispersive spectra (EDS) of undoped ZnO and 5 mol% of Ag:Co:ZnO nanocrystallites. EDS spectra of undoped ZnO having only two elements, Zn and O, indicates the purity of the ZnO sample and that an additional Co, Ag elements exists in Ag: Co: ZnO nanocrystals. Quantitative analysis of the dopants atomic concentration in ZnO (atom %) is listed in Table 2. The relative error of accuracy is less than ±3mol%. It can be found that the Ag content increases from 0.13% to 1.23%, based on the Ag doping levels (*chemical composition of Co =1.37 atom% was detected by EDS, for constant Co = 5 mol %).

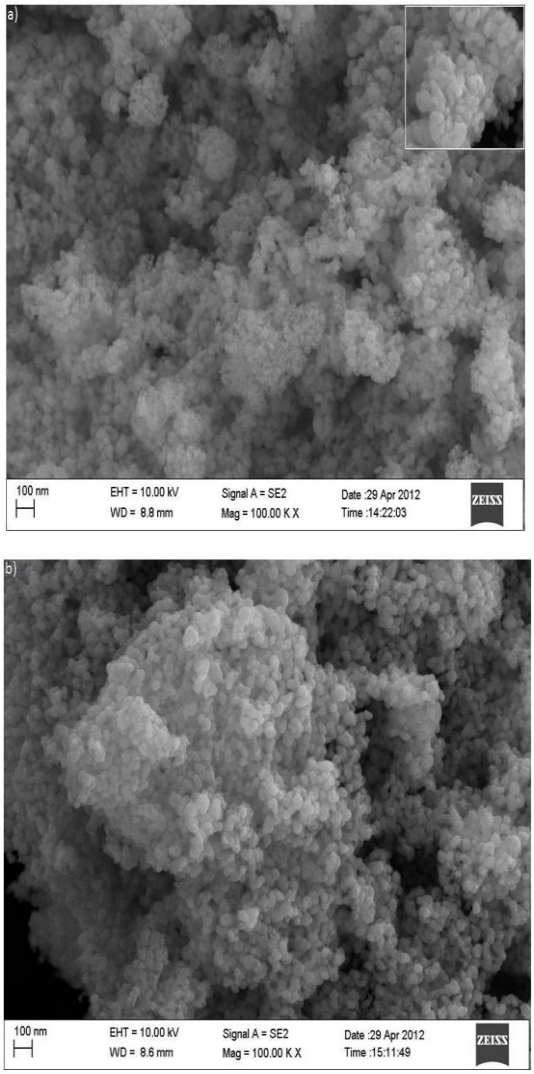

Fig. 2. FE-SEM images of: (a) Undoped ZnO, (b) 5 mol% of Ag + 5 mol% of Co doped ZnO nanoparticles.

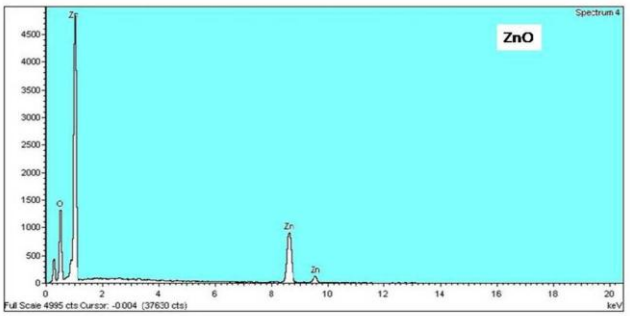

Fig. 3(a)

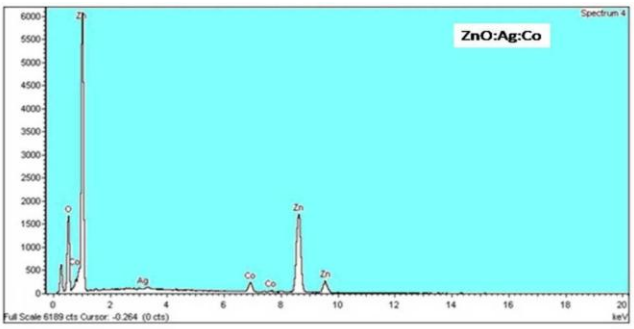

Fig. 3(b)

Fig. 3. EDAX Spectrum of: (a) Pure ZnO (b) 5 mol% of Ag, Co doped ZnO nanoparticles (ZnO: Ag: Co).

Table 2. Dopant concentration in ZnO measured by EDS (EDAX) method.

Composition (atom %)	Ag doping levels (mol %)					
	0	1	2	3	4	5
Zn	36.26	42.04	42.11	34.53	34.61	44.30
O	63.74	56.46	56.15	63.34	63.09	53.10
Ag	—	0.13	0.37	0.76	0.93	1.23
Co*	—	1.37	1.37	1.37	1.37	1.37

3.3 Optical studies of the pure ZnO and $Zn_{1-x}Ag_xCo_yO$ nanoparticles

UV-DRS spectra were recorded on a Varian UV−vis spectrometer in the wavelength range of 200 − 800 nm. The UV-vis diffuse absorption spectra of samples with different Ag concentration (by keeping Co = 5 mol %) were shown in Fig. 4. The band edge for pure ZnO sample appeared at 3.26 eV (380 nm), while the band edge of the co-doped ZnO samples shifted to longer wavelengths with

increasing Ag concentration, meanwhile the co-doped ZnO samples exhibits two types of bands which are present in UV-region and visible region. The strong UV-band present between 250-355 nm and strong absorption bands lies between 550 to 700 nm. In previous studies transition elements like silver, the excitonic absorption peak of undoped and silver doped samples appears around 260 nm, which fairly blue shifted from the absorption edge (Eg = 3.4 eV) of bulk ZnO, the excitonic absorption peak of undoped and silver doped samples become broad as temperature increases [12] and the excitonic absorption peaks observed at 262 nm and 284 nm due to ZnO nanoparticles shows blue shift [33, 36] and also 'Co' doped in ZnO nanoparticles has been observed the redshift of the band gap edge 'Eg' [37] and interpreted as mainly due to the sp-d exchange interactions between the band electrons and localized d electrons of the Co^{2+} ions substituting 'Zn' ions [38]. In this paper, we used two transitional elements such as Ag and Co, which are doped in ZnO nanoparticles. All co-doped ZnO samples exhibited two strong absorption bands like UV-band between 250-355 nm and visible band between 550 - 700 nm are observed. Three additional peaks at 550-700 nm appear in the spectra of the co-doped samples (see fig. 4), these peaks are attributed to the $^4A_2(F) \rightarrow {}^2E\ (G)$ (656 nm), $^4A_2(F) \rightarrow {}^4T_1\ (P)$ (612 nm), and $^4A_2(F) \rightarrow {}^2A_1(G)$ (565 nm) transitions respectively. These transitions are involved in the crystal field splitting of 3d levels of Co^{2+} in ZnO [39]. The blue shift and red shift can be observed clearly from Fig. 4, the absorbance is more for pure ZnO and decreased for co-doped ZnO samples, but the absorbance slightly increases from 2-5 mol% of Ag doped ZnO nanoparticles, which are having less absorbance than 1 mol% of 'Ag' doped ZnO samples. 1-5 mol% of 'Ag' doped (by keeping Co = 5 mol% as constant) ZnO samples exhibits UV-bands, among these 1 mol% of Ag doped ZnO shows highest degree of UV-band, but the intensity of the UV-bands raised with raise of dopant concentration of Ag from 2-5 mol%. On the other hand, we report that in the visible band Ag doped concentration increased from 1-5 mol% in ZnO samples (by keeping Co = 5 mol% as constant). Fig. 4 shows the highest degree of peaks for 1, 4, 5 mol% of Ag doped ZnO samples as compared to the data shows highest degree of absorption peaks for 3 mol% of Co^{2+} content doped ZnO, reported by Q. Xiao et. al [37]. Diffuse reflectance spectra of pure ZnO shows the absorption edge near 380 nm and all co-doped ZnO samples revealed characteristic absorption edge around 250-260 nm. Undoped and co-doped ZnO powders exhibits reflectance in the visible region. In the past study, reflectance of 'Ag' doped ZnO samples decreases with increase of 'Ag' concentration [19] and also reflectance of 'Co' doped ZnO nanoparticles decreases with increase of 'Co' concentration [40]. Here, we report that the Pure ZnO shows 61% reflectance [Fig. 5(a)], and in the co-doped ZnO samples, reflectance of the Ag doped ZnO samples increases with the increase in Ag concentration from 1 to 5 mol% (by keeping Co = 5 mol% as constant) such that 2 mol% of Ag doped ZnO shows 98% of reflectance and 5 mol% of Ag doped ZnO shows 82% of reflectance as shown in the Fig. 5(b). Band gap energy of the samples was estimated through the Kubelka- Munk treatment to their DRS spectra. Figure 6 represent the K-M plots for the undoped and Ag doped samples used to determine their band gap energies. The band gap energy decrease from 3.26 eV (pure ZnO) to ~2.88 eV (5 mol% Ag: Co: ZnO) with increase of 'Ag' concentration from 1 to 5 mol%. A small redshift was observed in the Ag doped ZnO samples as reported by R.S. Zeferino [19]. Where as we report, from Fig. 6, a redshift clearly observed for the ZnO samples doped with 1 to 5 mol% of Ag (by keeping Co = 5 mol% as constant).

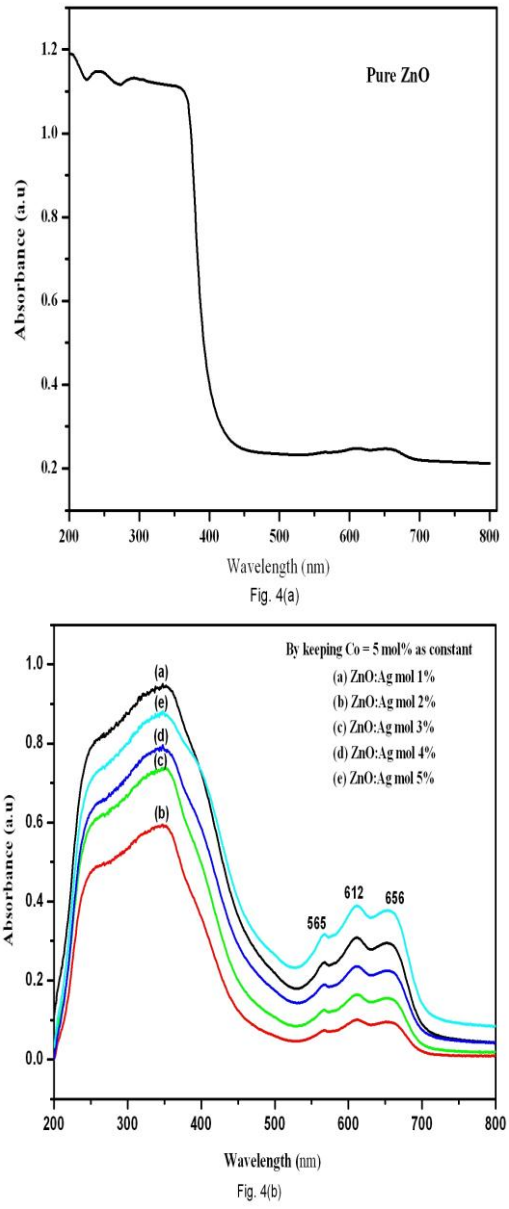

Fig. 4. UV–Vis diffuse absorption spectra of (a) Pure ZnO and (b) different concentrations of Ag doped ZnO powders (Keeping Co = 5.0 mol% as constant).

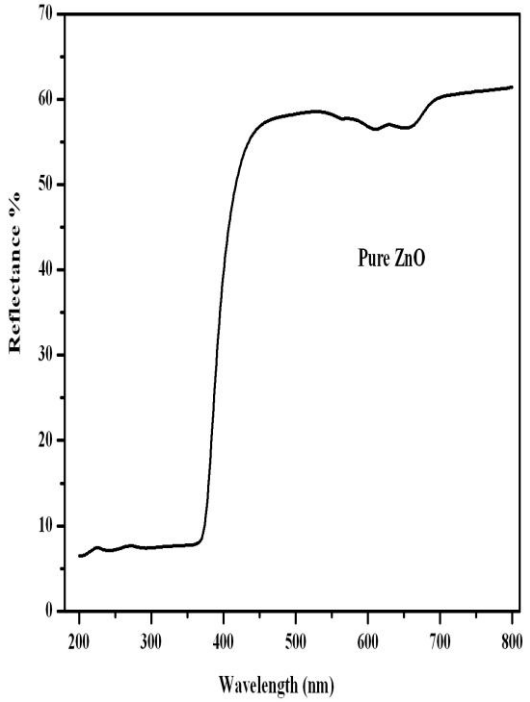

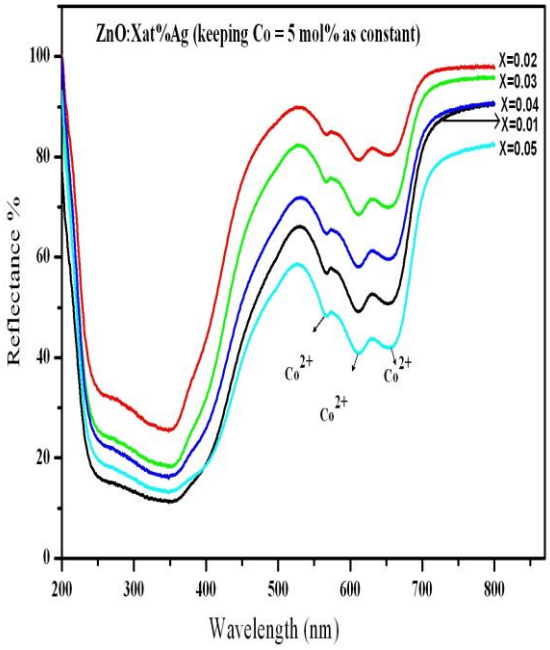

Fig. 5. Diffuse reflectance spectra of the (a) pure ZnO and (b) different co-doped (Ag, Co) Zn nanoparticles.

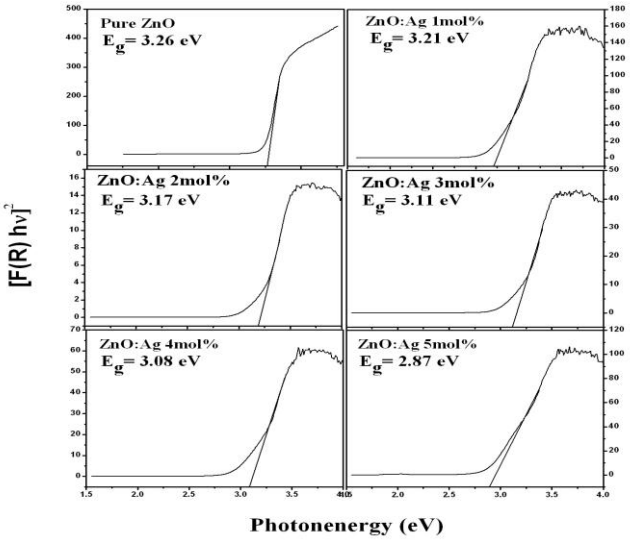

Fig. 6. Kubelka-Munk plots and band gap energy estimation for the undoped and Ag - doped ZnO nanoparticles (by keeping Co = 5mol %).

3.4 Photoluminescence studies of the pure ZnO and $Zn_{1-x}Ag_xCo_yO$ nanoparticles

Photoluminescence (PL) spectroscopy was used to study the luminescence behavior of pure and co-doped ZnO nanoparticles. Fig. 7(a) shows the PL spectrum of pure ZnO, and 5 mol% of Ag, and Co individually doped ZnO and Fig. 7(b) shows the PL spectrum of 1 to 5 mol% of Ag doped ZnO (by keeping Co = 5.0 mol% as constant) nanostructures. 1 to 5 mol% of Ag doped ZnO samples have excitation wavelength of 380 nm and have the energy 3.26 eV which is less than the direct band gap energy of ZnO (3.37eV). The PL spectra of pure ZnO has highest intensity than the intensity of Ag, Co doped ZnO nanostructures, and the intensity of visible emission is lesser for 5 mol% of silver doped ZnO than 5 mol% Co doped ZnO nanoparticles shown in Fig. 7(a). This is due to the most of the Ag^+ ions might have been incorporated into the ZnO lattice through substitution. The undoped and co-doped ZnO samples could exhibit a strong and wide PL signal in the range from 410 to 465 nm and two obvious PL peaks having wavelengths around at 420 nm and 444 nm are observed in the visible region. In the past, single element like 3 mol% of Co^{2+} ions of doped ZnO samples shows highest degree of intensity, reported by Q. Xiao et. al. [37] and also 2% of Ag doped ZnO samples shows highest degree of intensity as reported by R.S. Zeferino et. al [19]. But we report that the PL intensity is maxima for 5 mol% Ag doped ZnO samples and hence the PL intensity increases with rise of silver concentration from 1 to 5 mol% which is shown in the fig. 7(b), even though all these intensities are less than the PL intensity of pure ZnO. These PL signals were attributed to excitonic PL, which is mainly resulted from surface oxygen vacancies and defects of ZnO nanoparticles. It has been reported that the stronger the excitonic PL spectrum, the higher the content of surface oxygen vacancy and defect [41].

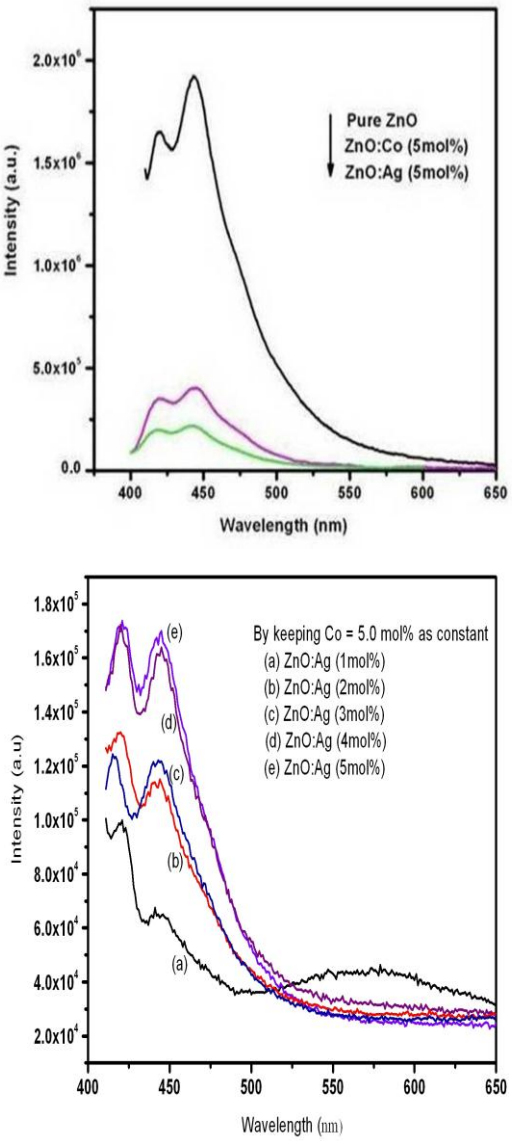

Fig. 7 PL spectra of the (a) pure ZnO and 5 mol% of Co and Ag doped ZnO nanoparticles, (b) 1 to 5 mol% Ag doped ZnO nanoparticles (Keeping Co = 5 mol % as constant).

4. Conclusions

Nanocrystals of pure and co-doped ZnO were successfully synthesized by using a chemical co-precipitation method. The crystalline structure, composition, morphology, and optical properties were determined by XRD, EDAX, FE-SEM, and DRS, respectively. XRD analysis shows that the prepared nanostructures have hexagonal crystal structure with pure ZnO phase. The evaluated average particle sizes increased and bond lengths, lattice parameters of nanoparticles are decreased with increase of 'Ag' dopant concentration from 1 to 5 mol%. Also, the band gap energy of ZnO is decreased from 3.26 eV to 2.87 eV with the increase of 'Ag' dopant concentration and optical absorption measurements indicate a strong blue shift and red-shift band edge upon increasing 'Ag' doping concentration. Blue emission was observed from photoluminescence Spectra and PL intensity increases with increase of Ag concentration from 1 to 5 mol%.

References

[1] S. C. Singh, R. Gopal, J. Phys. Chem. C **112**, 2812 (2008).
[2] D. D. Wang, J. H. Yang, L. L. Yang, Y. J. Zhang, J. H. Lang, M. Gao, Cryst. Res. Technol. **43**, 1041 (2008).
[3] D. Bao, H. Gu, A. Kuang, Thin Solid Films. **312**, 37 (1998).
[4] S. B. Majumdur, M. Jain, P. S. Dobal, R. S. Katiyar, Mater. Sci. Eng. B. **103**, 16 (2003).
[5] Y. Huang, M. Liu, Z. Li, Y. Zeng, S. Liu, Mater. Sci. Eng. B. **97**, 111 (2003).
[6] J. H. Lee, K. H. Ko, B. O. Park, J. Cryst. Growth. **247**, 119 (2003).
[7] D. R. Patil, L. A. Patil. Sensor. Actuat. B-Chem. **123**, 546 (2007).
[8] J. Lee, D. Lee, D. Lim, K. Yang, Thin Solid Films. **515**, 6094 (2007).
[9] L. Sikong, J. Damchan, K. Kooptarnond, S. Niyomwas, J. Sci. Technol. **30**, 385 (2008).
[10] J. M. Jang, C. R. Kim, H. Ryu, Razeghi, W. G. Jung, J. Alloys Compd. **463**, 503 (2008).
[11] S. Suwanboon, P. Amornpitoksuk, A. Raidoux, J. C. Tedenac, J. Alloys Compd. **462**, 335 (2008).
[12] R. Chauhan, A. Kumar, R. P. Chaudhary, Arch. Appl. Sci. Res. **2**, 378 (2010).
[13] X. H. Wang, B. Yao, D. Z. Zhen, Z. Z. Zhang, B. H. Li, Z. P. Wei, Y. M. Lu, D. X. Zhao, J. Y. Zhang, X. W. Fan, L. X. Guan, C. X. Cong, Solid State Commun. **141**, 600 (2007).
[14] C-J. Pan, H-C. Hsu, H-M. Cheng, C-Y. Wu, W-F. Hsieh, J. Solidstate. Chem. **180**, 1188 (2007).
[15] E. Pinel, P. Boutinaud, R. Mahiou, J. Alloys Compd. **374**, 165 (2004).
[16] Y. Inoue, M. Okamoto, Morimoto, Jpn. J. Appl. Phy. **45**, 4128 (2006).
[17] L .Irimpan, V. P. M. Nampoori, P. Radhakrishnan, Spectral Chemical Physics Letters **455**, 265 (2008).
[18] W. Xie, Y. Li, W. Sun, J. Haung, H. Xie, X. Zhao, J. Photochemistry And Photobiology A: Chemistry **216**, 149 (2010).
[19] R. S. Zeferino, M. B. Flores, U. Pal, J. Appl. Phys. **109**, 014308-1 (2011).
[20] C. Klingshirn, Phys. Status Solidi P **71**, 547 (1975).
[21] L. J. Zhuge, X. M. Wu, Z. F. Wu, X. M. Yang, X. M. Chen, Q. Chen, Mater. Chem. Phys. **120**, 480 (2010).

[22] F. Ochanda, K. Cho; D.Andala, T. C. Keane, A. Atkinson, W. E. Jones, Langmuir **25**, 7547 (2009).
[23] B. Panigrahy, M. Aslam, D. Bahadur, J. Phys. Chem. C **114**, 11758 (2010).
[24] M. L. Dinesha, H. S. Jayanna, S. Mohanty, S. Ravi, J. Alloys. Compd. **490**, 618 (2010).
[25] B. Sankara Reddy, S. Venkatramana Reddy, R. P. Vijaya Lakshmi, AIP Conf. Proc. **1447**, 431 (2012).
[26] B. D. Cullity, S. R. Stock, Elements of X-ray diffraction, Prentice Hall, New Jersey 2001.
[27] P. Li, S. Wang, J. Li, Y. Wei, Journal of Luminescence **132**, 220 (2012).
[28] X. Xu, C. Cao, Journal of Magnetism and Magnetic Materials **321**, 2216 (2009).
[29] F. Ahmed, S. Kumar, N. Arshi, M. S. Anwar, B. H. Koo, C. G. Lee, Microelectronic Engineering xxx (2011) xxx-xxx. (In press).
[30] P. M. Aneesh, C. T. Cherian, M. K. Jayaraj, T. Endo, JCS-Japan **118**, 333 (2010).
[31] S. B. Rana, P. Singh, A. K. Sharma, A. W. Carbonari, R. Dogra, J. Optoelectron. Adv. Mater. **12**, 257 (2010).
[32] M. A. Majeedkhan, M. Wasi Khan, M. Alhoshan, M. S. Alsalhi, A. S. Aldwayyan, Appl Phys. A **100**, 45 (2010).
[33] M. Nirmala, A. Anukaliani, Physica B **406**, 911 (2011).
[34] C. Karunakaran, V. Rajeswari, P. Gomathisankar, Superlattices and Microstructures **50**, 234 (2011).
[35] G. Srinivasan, R. T. Rajentra Kumar, J. Sol-gel Technol. **43**, 171 (2007).
[36] P. Kumbhakar, D. Singh, C. S. Tiwary, A. K Mitra, Chalcogen. Lett. **5**, 387 (2008).
[37] Q. Xiao, J. Zhang, C. Xiao, X. Tan, Materials Science and Engineering: B **142**, 121 (2007).
[38] Y. D. Kim, S. L. Cooper, M. V. Klein, B. T. Jonker. Phys. Rev. B **49**, 1732 (1994).
[39] X. Qiu, L. Li, G. Li, Appl. Phys. Lett. **88**, 114103 (2006).
[40] M. K. Patra, K. Manzoor, M. Manoth, S. R. Vadera, N. Kumar, J. Phys and Chem. of Solids **70**, 659 (2009).
[41] J. Liqiang, Q. Yichun, W. Baiqi, L. Shudan, J. Baojiang, Y. Libin, F. Honggang, S. Jiazhong F. Wei, F. Honggang, S. Jiazhong, Solar Energy Materials and Solar Cells **90**, 1773 (2006).

*Corresponding author: drsvreddy123@gmail.com